Journal of Solid State Chemistry 184 (2011) 3179–3184

Contents lists available at SciVerse ScienceDirect

Journal of Solid State Chemistry

journal homepage: www.elsevier.com/locate/jssc

Synthesis, structures and properties of new hybrid solids containing ruthenium complexes and polyoxometalates

Bangbo Yan *, Samantha A. Hodsdon, Yan-Fen Li, Christopher N. Carmichael, Yan Cao, Wei-Ping Pan

Department of Chemistry, Western Kentucky University, Bowling Green, KY 42101, USA

ARTICLE INFO

Article history:
Received 10 August 2011
Received in revised form
30 September 2011
Accepted 3 October 2011
Available online 8 October 2011

Keywords:
Ruthenium
Keggin cluster
Tungsten
Luminescence
Polyoxometalates

ABSTRACT

Two new organic–inorganic hybrid solids containing Keggin ions and ruthenium complexes have been synthesized and characterized by FT-IR, UV–vis, luminescence, X-ray, and TG analysis. In $KNa[Ru(bpy)_3]_2[H_2W_{12}O_{40}]\cdot 8H_2O$ (**1**), the $[Ru(bpy)_3]^{2+}$ (bpy=2,2′-bipyridine) complex ions are located in between the infinite one-dimensional double-chains formed by adjacent Keggin anions $[H_2W_{12}O_{40}]^{6-}$ linked through $\{KO_7\}$ and $\{NaO_6\}$ polyhedra, while in $K_6[Ru(pzc)_3]_2[SiW_{12}O_{40}]\bullet 12H_2O$ (**2**), the $[Ru(pzc)_3]^-$ (pzc=pyrazine-2-carboxylate) complex anions are confined by layered networks of the $[SiW_{12}O_{40}]^{4-}$ clusters connected by potassium ions. Both compounds exhibit three-dimensional frameworks through noncovalent interactions such as hydrogen bonds and anion$\cdots\pi$ interactions. Additionally, compound 1 shows strong luminescence at 604 nm in solid state at room temperature.

1. Introduction

Polyoxometalates are attracting increasing interest as building blocks of hybrid materials due to their large variety of applications such as catalysts [1], medicine[2], optoelectronics [3] and magnetism [4]. In the last decade, the chemistry of organic–inorganic hybrid solids containing polyoxotungstates has expanded rapidly [5,6]. On the other hand, ruthenium polypyridyl complexes have been extensively studied for their applications as photosensitizer in solar energy conversion and photoelectronic materials [7–10]. Recently, ruthenium heterocyclic ligand complex-based building blocks have been used for the synthesis of metal organic frameworks through the self-assembly [11]. However, the research on the interaction of polyoxotungstate anions with ruthenium complexes is rarely explored, except for a few reports on the interaction of polyoxotungstate anions with sensitizer $[Ru(bpy)_3]^{2+}$ (bpy=2,2′-bipyridine) in solutions in the last few years [12–16]. The fundamental structural study on the single-phase crystalline hybrid solid materials containing both Ru complex ions and polyoxotungstate anions remains particularly challenging, although thin films containing $[Ru(bpy)_3]^{2+}$ and polyoxotungstate anions [17], or solid compounds that built from the $[Ru(bpy)_3]^{2+}$ and polyoxotungstate anion building units have been reported [18]. It is clear that coordination or covalent bonds have played a significant role in the self-assembly of solid materials. However, in recent years, noncovalent interactions such as hydrogen bonding, π–π stacking, and anion–π interactions have been recognized as important bonding forces in forming supramolecular systems or metal organic framework materials. We are interested in the synthesis and structural study of transition metal complexes connected to polyoxotungstate anions through different ways such as coordination bonds, hydrogen bonds and ionic bonds [19]. In this study, we report the synthesis and characterization of two new hybrid solids $KNa[Ru(bpy)_3]_2[H_2W_{12}O_{40}]\cdot 8H_2O$ (**1**), and $K_6[Ru(pzc)_3]_2[SiW_{12}O_{40}]\cdot 12H_2O$ (**2**) (pzc=pyrazine-2-carboxylate), in which ruthenium heterocyclic ligand complexes are confined in space formed by one-/two-dimensional networks of polyoxometalates.

2. Material and methods

The reactions were carried out under hydrothermal/solvothermal autogenous pressure conditions using 3″ × 4″ Teflon bags in Teflon-lined stainless steel autoclave reactors. All chemicals were obtained from commercial sources and used without purification. No hazards were encountered in the experimental work reported. Reagents used were purchased from Alfa Aesar and used without further purification. Ultraviolet–visible (UV–vis) diffuse reflectance spectra were obtained using a Varian Cary 100 UV–vis spectrophotometer equipped with the DRA-CA-30 diffuse reflectance accessory. The infrared spectra were recorded from 400 to 4000 cm^{-1} on a Perkin Elmer Spectrum One FTIR spectrometer using KBr pellets. The thermogravimetric data were collected on a TA Q5000 TGA

* Corresponding author. Fax: +1 270 745 5361.
E-mail address: bangbo.yan@wku.edu (B. Yan).

0022-4596/$ - see front matter © 2011 Elsevier Inc. All rights reserved.
doi:10.1016/j.jssc.2011.10.005

instrument at a heating rate of 10 °C min^{-1} from room temperature to 800 °C in an air atmosphere. Powder X-ray analysis was performed on an ARL Thermo X-ray Diffraction instrument, and there are good matches between simulated powder pattern and experimental data. Fluorescence spectra were obtained by a Perkin Elmer LS55 fluorescence spectrophotometer. The emission spectra were obtained using an excitation wavelength of 450 nm.

2.1. Syntheses

$KNa[Ru(bpy)_3]_2[H_2W_{12}O_{40}]\cdot 8H_2O$ (**1**) was synthesized from a mixture of bpy, $3Na_2WO_4\cdot 9WO_3\cdot H_2O$, $RuCl_3\cdot xH_2O$ and H_2O. A typical synthesis is as follows: 1.0 mL aqueous solution containing 0.020 g $RuCl_3\cdot xH_2O$ was mixed thoroughly with 1.0 mL methanol solution containing bpy (0.029 g). Then, $3Na_2WO_4\cdot 9WO_3\cdot H_2O$ (0.141 g) was added and the pH of the resulting mixture was adjusted with 0.5 M KOH to approximately 10. The reaction mixtures were transferred to a Teflon bag, sealed and placed in a 45 mL reaction vessel, and heated in an oven at 90 °C for 48 h. Orange crystals were filtered and dried in air (yield: 0.034 g). FT-IR spectrum (KBr, cm^{-1}): 3492 (broad), 1624 (*m*), 1600 (*m*), 1445 (*m*), 1320 (*w*), 929 (*s*), 871 (*s*), 786 (*s*).

$K_6[Ru(pzc)_3]_2[SiW_{12}O_{40}]\cdot 12H_2O$ (**2**) was synthesized as follows: $H_4SiO_4\cdot 12WO_3\cdot xH_2O$ (0.103 g), and 1.0 mL methanol solution of pzc (0.027 g) were added to 1.0 mL aqueous solution containing 0.013 g $RuCl_3\cdot xH_2O$. The pH of this mixture was adjusted with 0.5 M KOH to approximately 8.5. The reaction mixtures were transferred to a Teflon bag, sealed and placed in a 45 mL reaction vessel, and heated in an oven at 105 °C for 48 h. Purple plate crystals were filtered and dried in air (yield: 0.053 g). FT-IR spectrum (KBr, cm^{-1}): 3457 (*s*), 1627 (*s*), 1606 (*s*), 1457 (*w*), 920 (*s*), 778 (*s*).

2.2. Crystallography

X-ray diffraction data for compounds **1** and **2** were collected on a Nonius kappa CCD diffractometer. Raw data were integrated, scaled, merged and corrected for Lorentz-polarization effects using the HKL-SMN package [20]. The structure was solved by direct methods and was refined against F^2 by weighted full-matrix least-squares calculations [21]. Non-hydrogen atoms were refined with anisotropic displacement parameters. Atomic scattering factors were taken from the International Tables for Crystallography [22]. Crystal data and relevant details of the structure determinations are summarized in Table 1 and selected geometrical parameters are given in Table 2. The CCDC reference numbers are 838,475 and 838,476.

3. Results and discussions

3.1. Crystal structure

3.1.1. Crystal structure of compound 1

The structure of **1** consists of Keggin cluster anion $[H_2W_{12}O_{40}]^{6-}$, water molecules, and charge balancing cations $[Ru(bpy)_3]^{2+}$, K^+ and Na^+. The classic $[H_2W_{12}O_{40}]^{6-}$ Keggin cluster ion [23] consists of twelve WO_6 octahedra with the four types of W–O bond lengths in normal ranges (Table 2). The bond valence sum calculations indicate oxygen atoms in the polyoxoanion have values between 1.60 and 2.06, normal for oxo groups, except that the triply bridging

Table 2
Selected bond lengths (Å) in **1** and **2.**

1		**2**	
W–O_t	1.704–1.744(6)	1.666–1.680(7)	
W–$O_{b/c}$	1.842–2.016(5)	1.780–2.061(7)	
W–O_a	2.126–2.302(5)	2.345–2.434(7)	
Si–O		1.60–1.66(1)	
Ru(1)–N(2)	2.052(7)	Ru(1)–N(3)	2.003(8)
Ru(1)–N(5)	2.057(7)	Ru(1)–N(1)	2.007(8)
Ru(1)–N(1)	2.059(7)	Ru(1)–N(5)	2.010(8)
Ru(1)–N(6)	2.061(7)	Ru(1)–O(27)	2.085(7)
Ru(1)–N(4)	2.062(7)	Ru(1)–O(23)	2.085(7)
Ru(1)–N(3)	2.067(6)	Ru(1)–O(25)	2.091(7)
Ru(2)–N(9)	2.046(7)		
Ru(2)–N(7)	2.050(7)		
Ru(2)–N(8)	2.059(7)		
Ru(2)–N(10)	2.059(7)		
Ru(2)–N(11)	2.061(7)		
Ru(2)–N(12)	2.067(7)		

Table 1
Crystal data and structure refinements for **1** and **2**

	1	2
Formula	$C_{60}H_{66}KN_{12}NaO_{48}Ru_2W_{12}$	$C_{15}H_{21}N_6K_3O_{32}RuSiW_6$
Mol. wt.	4193.68	2146.9
Crystal system	Monoclinic	Triclinic
Space group	$P2_1/n$	$P\bar{1}$
a (Å)	13.5339(1)	11.886(2)
b (Å)	26.9360(1)	12.206(2)
c (Å)	23.7255(1)	16.128(3)
α (deg.)		74.40(3)
β (deg.)	92.3155(2)	89.43(3)
γ (deg.)		61.46(3)
V (Å^3)	8642.05(8)	1960.2(7)
Z	4	2
ρ (Mg/m^3)	3.223	3.657
Abs. coeff. (mm^{-1})	16.39	18.36
Abs. correction	Multi-scan	Multi-scan
Wavelength (Å)	0.7103	0.7103
Temperature (K)	92.0(2)	92.0(2)
Reflections collected/unique [R_{int}]	19840 [0.125]	38,993[0.0467]
Goodness-of-fit (F^2)	1.068	1.060
Final *R* indices [$I>2\sigma(I)$]	$R_1=0.0346$, w$R_2=0.0778$	$R_1=0.0424$, w$R_2=0.115$
R indices (all data)	$R_1=0.0507$, w$R_2=0.0856$	$R_1=0.0508$, w$R_2=0.120$

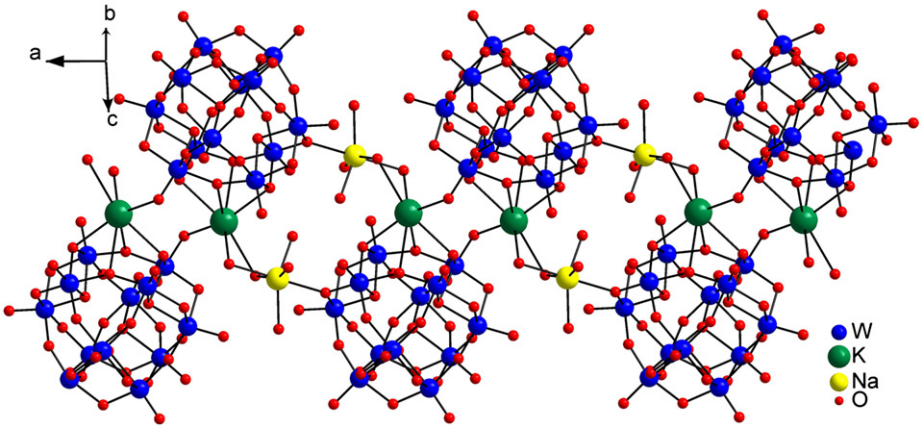

Fig. 1. Ball-and-stick representation of the one-dimensional double-chain in **1**.

Table 3
Hydrogen-bond geometry (Å, deg.) for compound **1**.

D–H···A	*d*(D–H)	*d*(H···A)	*d*(D···A)	∠DHA
C(3)–H(3)···O(19)#1	0.95	2.39	3.10(1)	131
C(11)–H(11)···O(3)#2	0.95	2.39	3.30(1)	160
C(17)–H(17)···O(5)#3	0.95	2.51	3.12(1)	122
C(20)–H(20)···O(1)	0.95	2.19	3.10(1)	161
C(24)–H(24)···O(40) #4	0.95	2.49	3.28(1)	140
C(27)–H(27)···O(32) #4	0.95	2.52	3.18(1)	127
C(34)–H(34)···O(15)	0.95	2.54	3.14(1)	121
C(37)–H(37)···O(2)	0.95	2.40	3.07(1)	127
C(40)–H(40)···O(21) #4	0.95	2.54	3.28(1)	135
C(44)–H(44)···O(29) #5	0.95	2.43	3.31(1)	155
C(47)–H(47)···O(16) #5	0.95	2.54	3.27(1)	134
C(50)–H(50)···O(20)#4	0.95	2.42	3.18(1)	136
C(53)–H(53)···O(18)#6	0.95	2.45	3.38(1)	166

D=donor, A=acceptor.Symmetry transformations used to generate equivalent atoms: #1: $1-x, 1-y, 1-z$; #2: $1/2+x, 3/2-y, -1/2+z$; #3: $1+x, y, z$; #4, $1/2-x, 1/2+y, 3/2-z$; #5: $3/2-x, 1/2+y, 3/2-z$; #6: $1/2+x, 3/2-y, 1/2+z$.

O(13) and O(26) atoms have a sum of 1.14/1.15 [24]. This indicates that these two oxygen atoms should be protonated and that the cluster unit in **1** should be $[H_2W_{12}O_{40}]^{6-}$ [25].

The remarkable structural feature of **1** is that adjacent Keggin anions are linked through $\{KO_7\}$ and $\{NaO_6\}$ polyhedra to form an infinite one-dimensional double-chain parallel to the *a*-axis as shown in Fig. 1. There are one crystallographically unique sodium site (Na(1)) and one potassium site (K(1)). K(1) is seven coordinated (K···O=2.687–3.116(8) Å) by two water molecules, one terminal oxo group of a Keggin ion, and four bridging oxo groups from another Keggin ion. The sodium ion Na(1) is six coordinated (Na···O=2.29–2.54(1) Å) to two bridging oxo groups of a Keggin ion and four water molecules. The double chain can also be viewed as: two Keggin ions are liked by two K^+ ions to form a dimer, and the neighboring dimers are linked by sodium ions to form infinite double chains along the *a*-axis. The double chains are arranged into a layer parallel to the *ac* plane, with $[Ru(bpy)_3]^{2+}$ located in between the layers.

There are extensive CH···H hydrogen bonds between $[Ru(bpy)_3]^{2+}$ and $[H_2W_{12}O_{40}]^{6-}$ in **1**. Some of the CH···O interactions are listed in Table 3. These interactions involve both terminal and bridged oxo groups of Keggin ions. Each $[H_2W_{12}O_{40}]^{6-}$ is surrounded by eight $[Ru(bpy)_3]^{2+}$ ions, which are located on one side of the anion. The other side of the $[H_2W_{12}O_{40}]^{6-}$ connected to other four units of $[H_2W_{12}O_{40}]^{6-}$ by K or Na ions. Each $[Ru(bpy)_3]^{2+}$ ions of Ru(1) connected to four $[H_2W_{12}O_{40}]^{6-}$ units by CH···O contacts (Fig. 2a), while the Each $[Ru(bpy)_3]^{2+}$ ions of Ru(2) connects to five $[H_2W_{12}O_{40}]^{6-}$ anions (Fig. 2b).

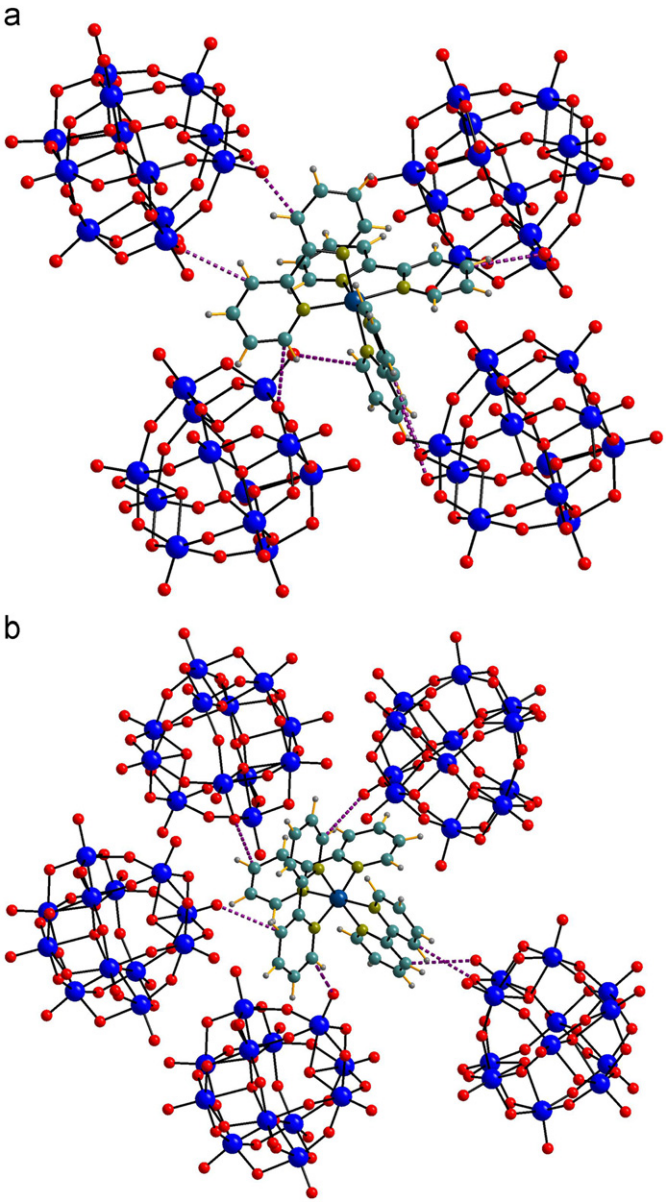

Fig. 2. The C–H···O hydrogen bonding in **1**: (a) the complex ion $[Ru(bpy)_3]^{2+}$ containing Ru(2) linked to four Keggin units through hydrogen bonding and (b) the complex ion $[Ru(bpy)_3]^{2+}$ containing Ru(1) connected to five Keggin units through hydrogen bonding.

There is an unusual interaction between W=O groups of the POM and the π-system of bpy ligands of the $[Ru(bpy)_3]^{2+}$ complex ion (Fig. 3). The terminal oxygen atoms (O(1), O(3), O(22), and O(23)) are oriented toward the π-faces of bpy ligands, with the separation distances between the terminal oxygen atoms and the centroid of the bpy ring range from 2.847 to 3.210(7) Å. The angles of the O···centroid axis to the plane of the different pyridine rings are 74.7 for O(1), 83.5 for O(3) and 81.4 for O(23). This indicates a significant anion···π interaction between Keggin anions and $[Ru(bpy)_3]^{2+}$, which is responsible for the formation and strengthening of the 3D assembly. The existence of anion···π interactions has been observed in some compounds recently [26]. Theoretical study suggests π–electron deficient aromatic rings such as heteroaromatics 1,3,5-triazine are energetically favorable to form anion···π interactions [27]. The $[H_2W_{12}O_{40}]^{6-}$ Keggin cluster ions and $[Ru(bpy)_3]^{2+}$ ions form 1D chains through the anion···π interaction.

In the structure of **1**, there are two unique Ru(II) sites, each of which showing a distorted octahedral coordination geometry and bonding to three bpy ligands with the Ru–N bond lengths in the range of 2.047(2)–2.058(2) Å. Those bond distances are comparable to the reported values and in normal range [28]. The two Ru complexes are enantiomers. Each enantiomer is packed into columns along the *a*-axis (Fig. 4). Adjacent $[Ru(bpy)_3]^{2+}$ units within a column show no direct interactions with the Ru–Ru distance of 13.53 Å (one unit length of the *a*). However, Ru complexes from neighboring columns form puckered layers along the *ac* plane through multiple aryl embraces [29], with nearest neighboring Ru–Ru distance at 7.995–8.832 Å. Each double chain of Keggin ions is surrounded by eight rows of $[Ru(bpy)_3]^{2+}$ complex ions. The negative charge on α-$[H_2W_{12}O_{40}]^{6-}$ is balanced by K^+, Na^+ and $[Ru(bpy)_3]^{2+}$. The oxidation state of ruthenium is 2+ in this compound as evident from the orange red color and the UV–vis spectra (see below). Normally, $[Ru(bpy)_3]^{3+}$ complex containing compound has dark green color [30]. Thus, the ruthenium(III) has been reduced to ruthenium(II) by methanol under sovolthermal conditions.

3.1.2. *Crystal structure of compound* ***2***

The single-crystal structure determination of **2** reveals that its asymmetric unit consists of one half Keggin anion $[SiW_{12}O_{40}]^{4-}$, one $[Ru(pzc)_3]^-$ anion, three K^+ cation, and six lattice water molecules.

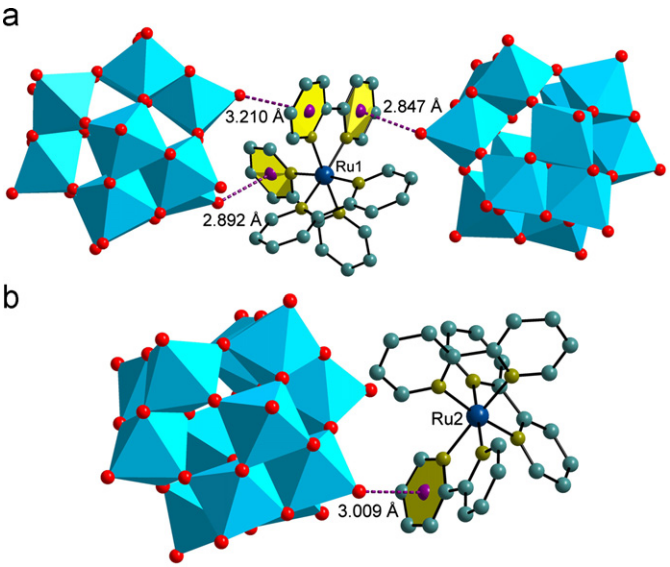

Fig. 3. The anion···π interactions in **1**: (a) the bpy ligands of complex ion $[Ru(bpy)_3]^{2+}$ containing Ru(1) form three anion···π interactions with two Keggin units. (b) The bpy ligands of complex ion $[Ru(bpy)_3]^{2+}$ containing Ru(2) Form one anion···π interaction with one Keggin unit.

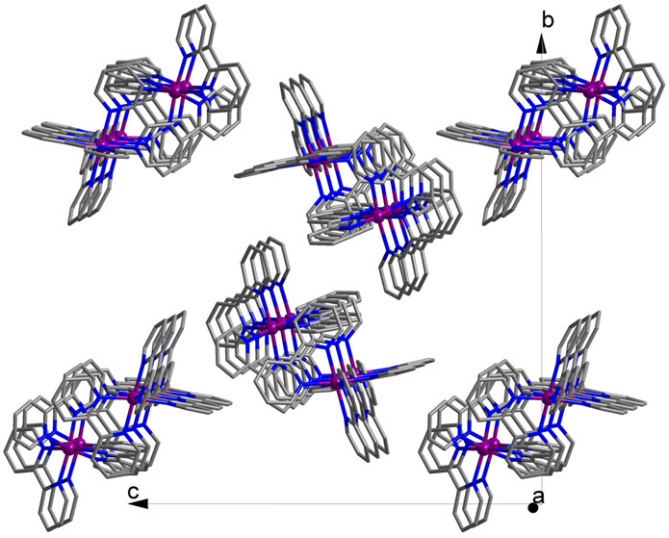

Fig. 4. The packing view of the $[Ru(bpy)_3]^{2+}$ in compound **1**. The Ru–Ru distance of adjacent $[Ru(bpy)_3]^{2+}$ units within a column is of 13.53 Å.

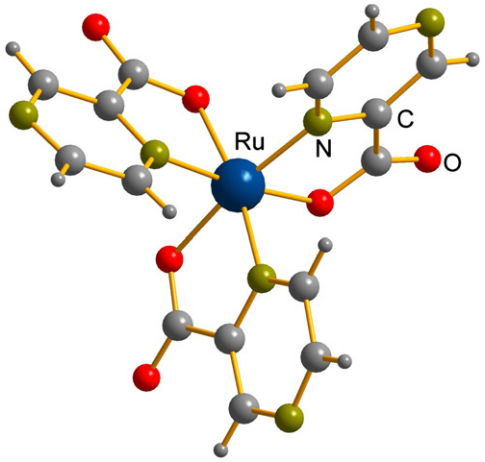

Fig. 5. The complex ion $[Ru(pzc)_3]^-$ in compound **2**.

At the center of the $[SiW_{12}O_{40}]^{4-}$ anion, the SiO_4 tetrahedron is disordered over two positions related by an inversion center at the site of Si atom (Si–O distances are in the range of 1.60(1)–1.66(1) Å). W–O distances are similar to those of **1**. The bond valence calculation for W atoms showed that their oxidation state is +6. An interesting feature of compound **2** is that it contains an anionic Ru complex $[Ru(pzc)_3]^-$ (Fig. 5). In this complex, the Ru(II) ion coordinates to three nitrogen atoms and three oxygen atoms from three pzc ligands and forms distorted octahedral coordination geometry $\{RuO_3N_3\}$. All the three oxygen atoms and three nitrogen atoms are in the *facial* positions. The O donor of one pzc is *trans* to the N donor of the other, with the *trans* angles around 170°. Bond length for Ru–N is in the range of 2.003(8)–2.010(8) Å and Ru–O bond lengths (2.085(7) × 2 and 2.091(7) Å). The Ru–N bond lengths are shorter than those in $[Ru(bpy)_3]^{2+}$, indicating strong $(d\pi)Ru^{II} \rightarrow (p\pi^*)$pyrazine(pzc) back-donation. To the best of our knowledge, no ruthenium complex of $[Ru(pzc)_3]^-$ has been reported so far.

The striking structural feature of **2** is that the $[SiW_{12}O_{40}]^{4-}$ clusters are linked through K(2) ions into a two-dimensional network parallel to the *ab* plane (Fig. 6). Each K^+ ion bonds to one water molecule and three terminal oxygen atoms from three different clusters. The K–O distance is in the range of

2.790–2.871 Å. The $[Ru(pzc)_3]^-$ anions are located in between the layers formed by the cluster ions and K^+ cations. Two $[Ru(pzc)_3]^-$ units linked by two K(1) ions and two K(3) ions to form a dimer $\{K_4[Ru(pzc)_3]_2\}$. The K(1) ion bonds to two oxygen atoms from different pzc ligands of a $Ru(pzc)_3]^-$ unit, and K(3) ion bonds to two oxygen atoms from one pzc of another $Ru(pzc)_3]^-$ unit. The K^+ cations of the dimer also connected to clusters through terminal oxygen atoms of the cluster. Thus the dimers link the layers into a three-dimensional framework. The crystal structure of **2** exhibits weak C–H···O interactions (C(4)···O(13) and C(6)···O(16)), and anion···π interactions (O(2)-pzc 3.40(1) and O(16)-pzc 3.24(1) Å).

3.2. UV–vis diffuse reflectance spectra

Fig. 7 shows the UV–vis diffuse reflectance spectra of compounds **1** and **2**. Compound **1** exhibits the characteristic metal-to-ligand charge transfer (MLCT) band of $[Ru(bpy)_3]^{2+}$ at 453 nm [31], and the π–π* transition of bpy ligand at about 290 nm, which is overlapped with the band of ligand-to-metal charge-transfer (LMCT) transitions for W(VI) (O→W) [32]. The MLCT band further confirmed the existence of Ru(II) in **1** and the reduction of Ru(III) to Ru(II) under the synthetic condition. The λ_{max} of MLCT band of compound **1** shows almost non-shift when compared with that of $[Ru(bpy)_3]^{2+}$ in aqueous solution (453 nm). When $[Ru(bpy)_3]^{2+}$ is included in solids such as zeolites or zirconium phosphate, the λ_{max} of its MLCT band is affected by its concentration in the solids [33]. A red shift is usually observed with increase of the concentration or loading of $[Ru(bpy)_3]^{2+}$. The red-shift could be explained by the interaction between $[Ru(bpy)_3]^{2+}$ ions. In the crystal structure of **1**, the interaction between $[Ru(bpy)_3]^{2+}$ ions are observed as multiple aryl embraces between bpy ligands, and the Ru–Ru distance is close to 8 Å. This interaction could prevent a red-shift of the MLCT band.

The UV–vis spectrum of compound **2** exhibits a broad band centered at 519 nm in visible range, which could be assigned to metal-to-ligand charge transfer (MLCT) band of $[Ru(pzc)_3]^-$. The bands at UV region are due to the (LMCT) transitions for W(VI) (O→W) and the π–π* transition of the pzc ligand.

3.3. IR

The IR spectrum of compound **1** shows a strong band around 3491 cm^{-1} due to the presence of coordinated water molecules. The strong bands at 929, 871, and 786 cm^{-1} (W–O) are typical of $[H_2W_{12}O_{40}]^{6-}$ [34]. Bands at 1320, 1445, 1624 cm^{-1} are characteristic absorption of bpy ligands.

The strong and broad peak around 3457 cm^{-1} in the IR spectrum of compound **2** can be attributed to the presence of coordinated water molecules. The strong band at 1627 cm^{-1} is assignable to the antisymmetric C=O stretching vibration of the coordinated carboxylate group, while the strong band at 788 cm^{-1} (Si–O) and 920 cm^{-1} (W–O) are typical of $[SiW_{12}O_{40}]^{4-}$ [35].

3.4. TGA

Thermogravimetric analysis of compound **1** exhibits a 3.9% weight loss in the range 40–370 °C, followed by 21.8% weight loss between 370 and 600 °C. These correspond to the loss of water molecules (calcd. 3.87%) and bpy (calcd. 22.34%). Compound **2** shows a similar thermogravimtric behavior: a weight loss of 5.0% up to 200 °C was observed, which can be attributed to the dissociation of crystalline water molecules (calcd. 5.04%). The weight loss of 15.9% at the range of 200–600 °C is corresponding to the loss of pzc ligands (calcd. 17.20%).

3.5. Luminescence spectra

The luminescence spectra of compound **1** as a suspension in water are shown in Fig. 8. Upon excitation at the λ_{max} (450 nm) of the MLCT band of the $[Ru(bpy)_3]^{2+}$, an emission centered around

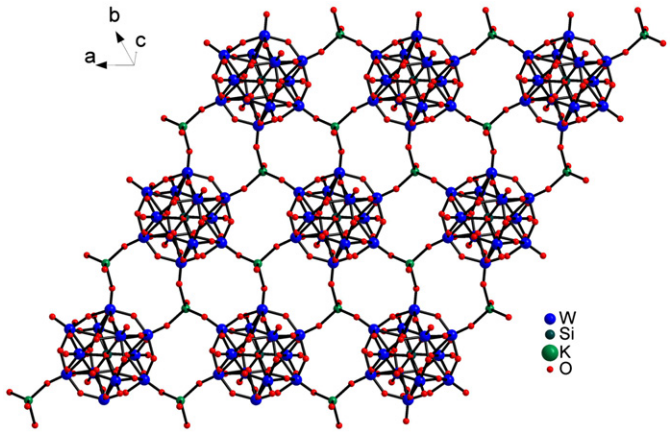

Fig. 6. The two-dimensional network formed by $[SiW_{12}O_{40}]^{4-}$ clusters and potassium ions in compound **2**.

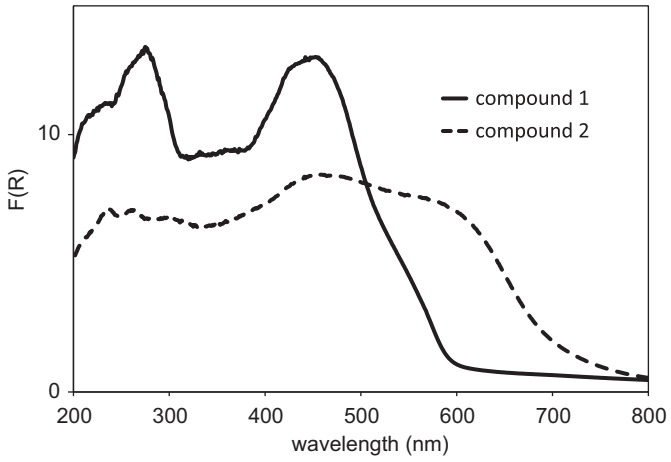

Fig. 7. The UV/vis spectrum of compounds **1** and **2**.

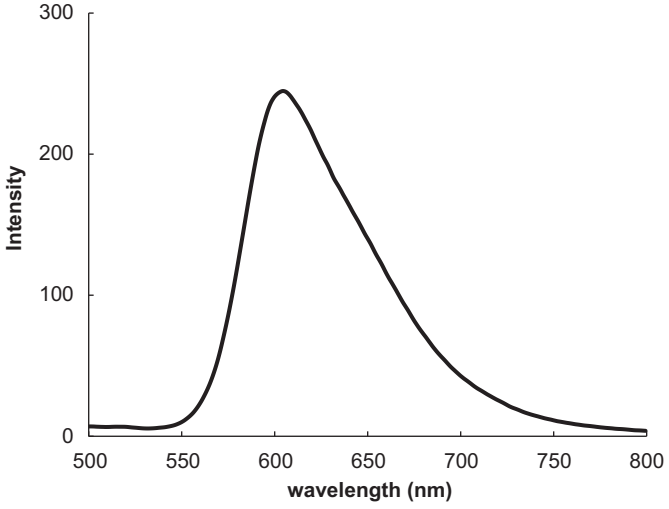

Fig. 8. The luminescence spectra of compound **1** excited at 450 nm.

604 nm was observed, which can be attributed to the emission from the triplet MLCT excited state (^{3}MLCT) to the ground state [36]. This emission shows a slight red-shift when compared with that in aqueous solution (around 600 nm at 293 K) [37], whereas no shift was observed in the absorption spectra. Normally, $[Ru(bpy)_3]^{2+}$ emits light of shorter wavelengths in a rigid matrix than in a fluid solution due to the Franck–Condon (unrelaxed) excited state is not completely stabilized or relaxed within its lifetime [38]. The red shift of in compound **1** could be due to the interactions between POM and $[Ru(bpy)_3]^{2+}$, which might destabilize the ground state of $[Ru(bpy)_3]^{2+}$. No luminescence has been observed in visible range for compound **2**. The possible reason for this is that pzc is a weaker field ligand than bpy, and this places the metal-centered antibonding e_g orbitals lower in energy than the ligand π^* orbitals. As a result, the singlet MLCT state of $[Ru(pzc)_3]^{1-}$ crossovers to a ligand field (LF) state, not a ^{3}MLCT state via intersystem crossing as in $[Ru(bpy)_3]^{2+}$. Thus the singlet MLCT states of $[Ru(pzc)_3]^{1-}$ deplete quickly via LF states and no luminescence can be detected.

4. Summary

We have made two new organic–inorganic compounds, in which the Ru complexes are immobilized with 1D or 2D polyoxometalate networks. In **1**, the $[Ru(bpy)_3]^{2+}$ complexes form layered network through multiple aryl embraces, and these layers are separated by 1D chains of Keggin ions. In **2**, the $[Ru(pzc)_3]^{-}$ complex anions are located in between the layers formed by the Keggin cluster ions and K^+ cations. In both compounds **1** and **2**, the noncovalent interactions between Keggin ions and the Ru complexes connected the two units into three-dimensional networks. The MLCT band of $[Ru(bpy)_3]^{2+}$ in **1** is not affected by these noncovalent interactions, while its luminescence is slightly affected. The $[Ru(bpy)_3]^{2+}$ and its derivatives show great potential applications in the fields of artificial photosynthesis, photovoltaics, photocatalysis and photoinduced water splitting due to interesting photochemical properties, and have been extensively investigated. We expect that modifying the ligands of $[Ru(bpy)_3]^{2+}$ will allow the synthesis of solid materials containing Ru complexes linked to POM through coordination bonds and these materials with enhanced photochemical properties.

Supporting information

Supporting Information Available: X-ray crystallographic file in CIF format, IR spectra, Powder XRD, and TGA. This material is available free of charge online.

Acknowledgment

We are grateful for financial support from the WKU internal grant, NSF EPSCoR (4800001974), and KY EPSCoR (RSF-030–06).

Appendix A. Supporting information

Supplementary data associated with this article can be found in the online version at doi:10.1016/j.jssc.2011.10.005.

References

[1] C.L. Hill, J. Mol. Catal. A: Chem. 262 (2007) 1–242.
[2] J.T. Rhule, C.L. Hill, D.A. Judd, R.F. Schinazi, Chem. Rev. 98 (1998) 327.
[3] D.E. Katsoulis, Chem. Rev. 98 (1998) 359.
[4] J.M. Clemente-Juan, E. Coronado, Coord. Chem. Rev. 193–195 (1999) 361 and references therein.
[5] A. Dolbecq, E. Dumas, C.R. Mayer, P. Mialane, Chem. Rev. 110 (2010) 6009–6048.
[6] (a) J.-X. Lin, J. Lu, H.-X. Yang, R. Cao, Cryst. Growth Des. 10 (2010) 1966–1970;
(b) H. Jin, Y. Qi, E. Wang, Y. Li, X. Wang, C. Qin, S. Chang., Cryst. Growth Des. 6 (2006) 2693–2698;
(c) C. Ritchie, T. Boyd, D.-L. Long, E. Ditzel, L. Cronin, Dalton Trans. (2009) 1587–1592;
(d) L. Yuan, C. Qin, X. Wang, Y. Li, E. Wang, Dalton Trans. (2009) 4169–4175;
(e) J. Sha, J. Peng, Y. Lan, Z. Su, H. Pang, A. Tian, P. Zhang, M. Zhu, Inorg. Chem. 47 (2008) 5145–5153;
(f) J.-P. Wang, X.-D. Du, J.-Y. Niu, J. Solid State Chem. 180 (2007) 1347–1352;
(g) E. Burkholder, V. Golub, C.J. O'Connor, J. Zubieta, Inorg. Chem. Commun. 7 (2004) 363–366;
(h) S. Reinoso, P. Vitoria, L. Lezama, A. Luque, J.M. Gutierrez-Zorrilla, Inorg. Chem. 42 (2003) 3709–3711;
(i) J.-W. Zhao, B. Li, S.-T. Zheng, G.-Y. Yang, Cryst. Growth Des. 7 (2007) 2658–2664;
(j) B.-Z. Lin, L.W. He, B.-H. Xu, X.-L. Li, Z. Li Z., P.-D. Liu, Cryst. Growth Des. 9 (2009) 273–281;
(k) P.-Q. Zheng, Y.-P. Ren, L.-S. Long, R.-B. Huang, L.-S. Zheng, Inorg. Chem. 44 (2005) 1190–1192.
[7] K. Kalyanasundaram, Coord. Chem. Rev. 46 (1982) 159–244.
[8] V. Balzani, G. Bergamini, F. Marchioni, P. Ceroni, Coord. Chem. Rev. 250 (2006) 1254–1266.
[9] C. Creutz, N. Sutin, Proc. Natl. Acad. Sci. USA 72 (1975) 2858.
[10] T.J. Meyer, Pure Appl. Chem. 58 (1986) 1193–1206.
[11] C.A. Kent, B.P. Mehl, L. Ma, J.M. Papanikolas, T.J. Meyer, W. Lin, J. Am. Chem. Soc. 132 (2010) 12767–12769.
[12] M.K. Seery, N. Fay, T. McCormac, E. Dempsey, R.J. Forstera, T.E. Keyes, Phys. Chem. Chem. Phys. 7 (2005) 3426–3433.
[13] M.K. Seery, L. Guerin, R.J. Forster, E. Gicquel, V. Hultgren, A.M. Bond, A.G. Wedd, T.E. Keyes, J. Phys. Chem. A 108 (2004) 7399–7405.
[14] N. Fay, V.M. Hultgren, A.G. Wedd, T.E. Keyes, R.J. Forster, D. Leaned, A.M. Bond, Dalton Trans. (2006) 4218–4227.
[15] L. Ruhlmann, C. Costa-Coquelard, J. Hao, S. Jiang, C. He, L. Sun, I. Lampre, Can. J. Chem. 86 (2008) 1034–1043.
[16] Y.V. Geletii, B. Botar, P. Kogerler, D.A. Hillesheim, D.J. Musaev, C.L. Hill, Angew. Chem. Int. Ed. 47 (2008) 3896–3899.
[17] (a) T. Dong, H. Ma, W. Zhang, L. Gong, F. Wang, C. Li, J. Colloid Interface Sci. 311 (2007) 523–529;
(b) H. Ma, J. Peng, Y. Chen, Y. Feng, E. Wang, J. Solid State Chem. 177 (2004) 3333–3338.
[18] (a) Z. Han, E. Wang, G. Luan, Y. Li, C. Hu, P. Wang, N. Hu, H. Jia, Inorg. Chem. Commun. 4 (2001) 427–429;
(b) L.H. Bi, B. Li, L.X. Wu, J. Solid State Chem. 182 (2009) 1401–1407;
(c) L.H. Bi, B. Li, L.X. Wu, Inorg. Chem. Commun. 11 (2008) 1187;
(d) L.H. Bi, G.F. Hou, Y.Y. Bao, B. Li, L.X. Wu, Z.M. Gao, T. McCormac, S.S. Mal, M.H. Dickman, U. Kortz, Eur. J. Inorg. Chem. 34 (2009) 5259–5266;
(e) J. Song, Z. Luo, H. Zhu, Z. Huang, T. Lian, A.L. Kaledin, D.G. Musaev, S. Lense, K.I. Hardcastle, C.L. Hill, Inorg. Chim. Acta 363 (2010) 4381–4386.
[19] (a) B.B. Yan, Y.F. Li, H.Y. Zhao, W.P. Pan, S. Parkin, Inorg. Chem. Commun. 12 (2009) 1139;
(b) Y.F. Li, D.G. Hubble, R.G. Miller, H.Y. Zhao, W.P. Pan, S. Parkin, B. Yan, Polyhedron 29 (2010) 3324–3328;
(c) A.M. Smelser, Y.F. Li, C.N. Carmichael, H.Y. Zhao, W.P. Pan, S. Parkin, B.B. Yan, Inorg. Chim. Acta 375 (2011) 122.
[20] Z. Otwinowski, W. Minor, Methods in Enzymology, vol. 276, in: C.W. Carter Jr., R.M. Swet (Eds.), Macromolecular Crystallography part A, Academic Press, 1997, pp. 307–326.
[21] G.M. Sheldrick, Acta Crystallogr. A64 (2008) 112–122.
[22] Th. Hahn (Ed.), International Tables for Crystallography, vol. C, Kluwer Academic Publishers, Holland.
[23] J.F. Keggin, Nature 131 (1933) 908–909.
[24] D. Brown, D. Altermatt, Acta Crystallogr. Sect. B 41 (1985) 244–247.
[25] M.T. Pope, G.M. Varga Jr, Chem. Commun. (1966)653 (1966).
[26] (a) S. Demeshko, S. Dechert, F. Meyer, J. Am. Chem. Soc. 126 (2004) 4508;
(b) P. de Hoog, P. Gamez, I. Mutikainen, U. Turpeinen, J. Reedijk, Angew. Chem. Int. Ed. 43 (2004) 5815–5817.
[27] M. Mascal., A. Armstrong, M.D. Bartberger, J. Am. Chem. Soc. 124 (2002) 6274.
[28] (a) W. Dong, Y. Ou-Yang, H.B. Song, D.Z. Liao, Z.H. Jiang, S.P. Yan, P. Cheng, Inorg. Chem. 45 (2006) 1168–1172;
(b) F. Pointillart, C. Train, M. Gruselle, F. Villain, H.W. Schmalle, D. Talbot, P. Gredin, S. Decurtins, M. Verdaguer, Chem. Mater. 16 (2004) 832–841.
[29] Dance, M. Scudder, J. Chem. Soc. Dalton Trans. (1998) 1341–1350.
[30] M. Biner, H.B. Burgi, A. Ludi, C. Rohr, J. Am. Chem. Soc. 114 (1992) 5197–5203.
[31] E.M. Kober, T.J. Meyer, Inorg. Chem. 21 (1982) 3967.
[32] E.I. Ross-Medgaarden, I.E. Wachs, J. Phys. Chem. C 111 (2007) 15089–15099.
[33] (a) A.A. Marti, J.L. Colon, Inorg. Chem. 49 (2010) 7298–7303;
(b) N.B. Castagnola, P.K. Dutta, J. Phys. Chem. B 105 (2001) 1537–1542.
[34] K. Nomiya, M. Miwa, R. Kobayashi,and, M. Aiso, Bull. Chem. Soc. Jpn. 44 (1981) 2983–2987.
[35] C. Rocchiccioli-Deltcheff, M. Fournier, R. Franck, R. Thouvenot, Inorg. Chem. 32 (1983) 207–216.
[36] V. Juris, F. Balzani, S. Barigelletti, P. Campagna, A. Belser, Von Zelewsky, Coord. Chem. Rev. 84 (1988) 85.
[37] K. Kalyanasundaram, Coord. Chem. Rev. 46 (1982) 159–244.
[38] P. Innocenzi, H. Kozuka, T. Yoko, J. Phys. Chem. B 101 (1997) 2285–2291.